International Journal of Thermophysics, Vol. 22, No. 6, November 2001 (© 2001)

Determination of the Fundamental Frequencies of Fluorochloro-Derivatives of Ethane and Its Application to Calculate Ideal Gas Heat Capacities

M. Speis,[1] U. Delfs,[2] and K. Lucas[3, 4]

Received October, 18, 2000

Quantum mechanical calculations for all fluorochloro-derivatives of ethane were performed. It was shown that the B3LYP/cc-pVDZ density functional method and single-point MP2/cc-pVTZ calculations lead to an accuracy of the molecular data that is sufficient for prediction of ideal gas heat capacities. Finally, reliable experimental heat capacity data reveal that an uncertainty of the heat capacity calculations of ±1.5% or less is achieved.

KEY WORDS: halogenated ethanes; heat capacity; ideal gas; molecular structure; vibrational frequencies.

1. INTRODUCTION

It was pointed out in Refs. 1 and 2 that the combination of quantum mechanical calculations and statistical thermodynamics [3] provides a suitable path for the prediction of molecular properties and heat capacities. Only fundamental physical constants and the structural formula enter into the calculations. From the results obtained for all fluorochloro-derivatives of methane, it was concluded [2] that the B3LYP density functional method [4] with the cc-pVDZ basis set [5] is a rational route to the ideal gas heat capacity of the halocarbons investigated so far. Here we present the results we obtained from this method for the fluorochloro-derivatives of ethane.

---

[1] GETISmbH, Königsstr. 72, D-47051 Duisburg, Germany.

[2] VDI-Gesellschaft Energietechnik, Graf-Recke-Str. 84, D-40239 Düsseldorf, Germany.

[3] Lehrstuhl für Technische Thermodynamik, RWTH Aachen, Schinkelstr. 8, D-52056 Aachen, Germany.

[4] To whom correspondence should be addressed. E-mail: lucas@ltt.rwth-aachen.de

0195-928X/01/1100-1813/0 © 2001 Plenum Publishing Corporation

2. IDEAL GAS HEAT CAPACITY OF ETHANE AND ITS DERIVATIVES

An N-atomic molecule possesses $3N$ degrees of freedom of motion. In the rigid rotator-harmonic oscillator approximation (RRHO) [3], the different modes of motion are independent of each other. For a nonlinear molecule three degrees of freedom are related to translation and three to external rotation. The remaining $3N-6$ internal modes are vibrations. For methane-like molecules all of these modes may be treated as harmonic oscillations. But for ethane and its derivatives, special attention has to be given to the particular mode of torsion. At low temperatures the atomic groups attached to the two carbon atoms oscillate around the connecting carbon–carbon axis at a low amplitude. If the temperature is increased, this oscillation changes into an internal rotation of the groups, which is affected by intramolecular forces, i.e., a hindered internal rotation occurs. In the limit of very high temperatures, which is equivalent to weak intramolecular forces, interactions become of less importance until a free internal rotation occurs.

Independent modes of motion lead to a heat capacity,

$$c_{\mathrm{p}}^{\mathrm{ig}} = R + c_{\mathrm{tr}}^{\mathrm{ig}} + c_{\mathrm{rot}}^{\mathrm{ig}} + c_{\mathrm{vib}}^{\mathrm{ig}} + c_{\mathrm{irot}}^{\mathrm{ig}} \tag{1}$$

where R denotes the molar gas constant and $c_{\mathrm{tr}}^{\mathrm{ig}} = c_{\mathrm{rot}}^{\mathrm{ig}} = \frac{3}{2}R$ are the constant contributions of translation and external rotation. The temperature dependence and characteristics of the individual molecules are included in the contributions of the internal modes of motion. Evaluation of the vibrational part to the heat capacity $c_{\mathrm{vib}}^{\mathrm{ig}}$ is reduced to $(3N-6)-1$ normal modes, because now the torsional mode is treated separately in the contribution of hindered internal rotation $c_{\mathrm{irot}}^{\mathrm{ig}}$. The contribution of hindered internal rotation

$$c_{\mathrm{irot}}^{\mathrm{ig}} = f(T, V_{\mathrm{ir}}(\varphi), I_{\mathrm{red}}) \tag{2}$$

has to be computed by solving the Schrödinger equation numerically or by means of tabulated values [3]. Only two limiting cases enable direct calculation. The first is the low-temperature case, where small oscillations occur, and the contribution may be evaluated from the vibrational formula. On the other hand, at high temperatures the limit of free internal rotation will be approached, which is $c_{\mathrm{irot,\ free}}^{\mathrm{ig}} = \frac{1}{2}R$. In the intermediate region the contribution of hindered internal rotation may exceed $1R$, which is the maximum contribution of one vibration. The magnitude of $c_{\mathrm{irot}}^{\mathrm{ig}}$ strongly depends on the intramolecular energy $V_{\mathrm{ir}}(\varphi)$, which is usually expressed as a Fourier-series expansion,

$$V_{\mathrm{ir}}(\varphi)=\tfrac{1}{2}\sum_{n}^{6} V_n[1-\cos(n\varphi)] \tag{3}$$

where φ is the torsional angle of the connecting CC-axis and V_n are the potential coefficients of the series expansion. The latter can be obtained from spectroscopy or from quantum mechanical calculations. Here we use quantum mechanics to eliminate any need for spectroscopic data.

To predict the heat capacity, the reduced moment of inertia of internal rotation I_{red} is required. If both rotating groups attached to each other show threefold symmetry, the reduced moment of inertia is easily calculated from the moments of inertia I_1, I_2 of the groups 1 and 2 with respect to the rotational axis [3],

$$I_{\mathrm{red}}=\frac{I_1 I_2}{I_1+I_2} \tag{4}$$

If at least one rotational group shows threefold symmetry, the reduced moment is expressed as

$$I_{\mathrm{red}}=I_1\left[1-I_1\left(\frac{\cos^2\alpha}{I_{\mathrm{A}}}+\frac{\cos^2\beta}{I_{\mathrm{B}}}+\frac{\cos^2\gamma}{I_{\mathrm{C}}}\right)\right] \tag{5}$$

with I_1 being the moment of the symmetrical group, I_{A}, I_{B}, and I_{C} the principal moments of inertia, and α, β, and γ the angles between the principal moments and the rotational axis [3].

3. RESULTS

For the series of the fluorochloro-derivatives of ethane, 55 constituent isomers exist. Some of them possess two, and some three isomers, which result from a rotation around the CC axis, i.e., rotational isomers, and, for one, even five rotational isomers. The latter is the chiral molecule 1,2-dichloro-1,2-difluoroethane. Therefore, a total of 92 isomers exists for the series of ethane. B3LYP/cc-pVDZ [4, 5] calculations were performed for all isomers using GAUSSIAN98 [6]. In the following we present the results only for those molecules for which experimental zero-pressure heat capacity data are available in the literature. The reader who is interested in the results for the other molecules is referred to Ref. 7. The results of molecular structure are given in Table I. The last column in Table I contains the reduced moment of inertia calculated from Eq. (5) for molecules

Table I. Molecular Geometry of Selected Fluorochloro-Derivatives of Ethane [r (pm), α (degree), I_{red} (10^{-40} g · cm^2)]

Molecule	Conformation	Molecular structure	I_{red}
C_2H_6	Conf = *ap* Sym = D_{3d}	$r_{CC} = 152.91$, $r_{CH} = 110.28$, $\alpha_{CCH} = 111.48$	2.644
CH_3–CHF_2	Conf = *ap* Sym = C_s	$r_{CC} = 1.5063$, $r_{CH3} = 1.1041$, $r_{CH4} = 1.1005$, $r_{CF5,6} = 1.3725$, $r_{CH7,8} = 1.1001$, $\alpha_{CCH3} = 114.00$, $\alpha_{CCH4} = 109.29$, $\alpha_{CCF5,6} = 110.14$, $\alpha_{CCH7,8} = 110.12$, $\alpha_{F5CF6} = 107.17$, $\alpha_{H7CH8} = 109.04$	5.070
CH_3–CF_3	Conf = *ap* Sym = C_{3v}	$r_{CC} = 1.5043$, $r_{CF} = 1.3532$, $r_{CH} = 1.0985$, $\alpha_{CCF} = 111.77$, $\alpha_{CCH} = 109.47$	5.198
CH_3–$CClF_2$	Conf = *ap* Sym = C_s	$r_{CC} = 1.5069$, $r_{CCl3} = 1.8167$, $r_{CH4} = 1.1008$, $r_{CF5,6} = 1.3531$, $r_{CH7,8} = 1.0977$, $\alpha_{CCCl3} = 111.92$, $\alpha_{CCH4} = 108.23$, $\alpha_{CCF5,6} = 111.14$, $\alpha_{CCH7,8} = 109.95$, $\alpha_{F5CF6} = 107.05$, $\alpha_{H7CH8} = 109.63$	5.275
CH_3–CCl_2F	Conf = *ap* Sym = C_s	$r_{CC} = 1.5114$, $r_{CF} = 1.3562$, $r_{CH4} = 1.0970$, $r_{CCl5,6} = 1.8112$, $r_{CH7,8} = 1.0999$, $\alpha_{CCF} = 110.35$, $\alpha_{CCH4} = 110.49$, $\alpha_{CCCl5,6} = 111.06$, $\alpha_{CCH7,8} = 108.82$, $\alpha_{Cl5CCl6} = 109.16$, $\alpha_{H7CH8} = 109.47$	5.318
CF_3–CH_2F	Conf = *ap* Sym = C_s	$r_{CC} = 1.5186$, $r_{CF3} = 1.3769$, $r_{CF4} = 1.3522$, $r_{CH5,6} = 1.1016$, $r_{CF7,8} = 1.3449$, $\alpha_{CCF3} = 109.88$, $\alpha_{CCF4} = 109.00$, $\alpha_{CCH5,6} = 108.59$, $\alpha_{CCF7,8} = 111.93$, $\alpha_{H5CH6} = 109.95$, $\alpha_{F7CF8} = 107.80$	26.784
CF_3–CH_2Cl	Conf = *ap* Sym = C_s	$r_{CC} = 1.5188$, $r_{CCl3} = 1.7943$, $r_{CF4} = 1.3542$, $r_{CH5,6} = 1.0971$, $r_{CF7,8} = 1.3435$, $\alpha_{CCCl3} = 112.25$, $\alpha_{CCF4} = 108.38$, $\alpha_{CCH5,6} = 108.80$, $\alpha_{CCF7,8} = 112.39$, $\alpha_{H5CH6} = 110.04$, $\alpha_{F7CF8} = 108.04$	42.048
CF_3–CHF_2	Conf = *ap* Sym = C_s	$r_{CC} = 1.5350$, $r_{CH} = 1.1023$, $r_{CF4} = 1.3378$, $r_{CF5,6} = 1.3554$, $r_{CF7,8} = 1.3444$, $\alpha_{CCH} = 110.57$, $\alpha_{CCF4} = 111.69$, $\alpha_{CCF5,6} = 108.94$, $\alpha_{CCF7,8} = 109.65$, $\alpha_{F5CF6} = 108.93$, $\alpha_{F7CF8} = 108.33$	56.502
CF_3–$CHClF$	Conf = *ap* Sym = C_1	$r_{CC} = 1.5365$, $r_{CF3} = 1.3464$, $r_{CCl4} = 1.7898$, $r_{CF5} = 1.3366$, $r_{CF6} = 1.3426$,$r_{CF7} = 1.3594$, $r_{CH8} = 1.0989$, $\alpha_{CCF3} = 108.74$, $\alpha_{CCCl4} = 110.94$, $\alpha_{CCF5} = 112.33$, $\alpha_{CCF6} = 110.26$, $\alpha_{CCF7} = 108.58$, $\alpha_{CCH8} = 109.44$, $\alpha_{F3CF5} = 108.35$, $\alpha_{F3CF6} = 108.12$, $\alpha_{Cl4CF7} = 110.22$, $\alpha_{Cl4CH8} = 107.74$, $\tau_{Cl4CCF3} = 179.82$	77.359
CF_3–$CClF_2$	Konf = *ap* Sym = C_s	$r_{CC} = 1.5525$, $r_{CCl} = 1.7855$, $r_{CF4} = 1.3403$, $r_{CF5,6} = 1.3423$, $r_{CF7,8} = 1.3364$, $\alpha_{CCCl} = 111.31$, $\alpha_{CCF4} = 108.94$, $\alpha_{CCF5,6} = 108.74$, $\alpha_{CCF7,8} = 110.55$, $\alpha_{F5CF6} = 108.57$, $\alpha_{F7CF8} = 109.23$	92.187

CF_3–$CHCl_2$	Conf = *ap* Sym = C_s	$r_{CC}=1.5393$, $r_{CH3}=1.0958$, $r_{CF4}=1.3361$, $r_{CCl5,6}=1.7894$, $r_{CF7,8}=1.3448$, $\alpha_{CCH3}=108.49$, $\alpha_{CCF4}=112.64$, $\alpha_{CCCl5,6}=110.40$, $\alpha_{CCF7,8}=109.60$, $\alpha_{Cl5CCl6}=111.97$, $\alpha_{F7CF8}=107.78$	98.033
$CClF_2$–$CHClF$	Conf = *ap* Sym = C_1	$r_{CC}=1.5413$, $r_{CCl3}=1.8017$, $r_{CCl4}=1.7957$, $r_{CF5}=1.3389$, $r_{CF6}=1.3443$,$r_{CF7}=1.3564$, $r_{CH8}=1.0981$, $\alpha_{CCCl3}=109.40$, $\alpha_{CCCl4}=110.10$, $\alpha_{CCF5}=111.45$, $\alpha_{CCF6}=109.56$, $\alpha_{CCF7}=109.40$, $\alpha_{CCH8}=109.74$, $\alpha_{Cl3CF5}=109.03$, $\alpha_{Cl3CF6}=108.71$, $\alpha_{Cl4CF7}=109.72$, $\alpha_{Cl4CH8}=107.55$, $\tau_{Cl4CCCl3}=179.12$	119.718
	Conf = +*sc* Sym = C_1	$r_{CC}=1.5438$, $r_{CCl3}=1.7947$, $r_{CCl4}=1.7880$, $r_{CF5}=1.3486$, $r_{CF6}=1.3394$, $r_{CF7}=1.3616$, $r_{CH8}=1.0982$, $\alpha_{CCCl3}=111.09$, $\alpha_{CCCl4}=111.75$, $\alpha_{CCF5}=107.79$, $\alpha_{CCF6}=111.43$, $\alpha_{CCF7}=107.61$, $\alpha_{CCH8}=109.84$, $\alpha_{Cl3CF5}=108.64$, $\alpha_{Cl3CF6}=109.76$, $\alpha_{Cl4CF7}=109.70$, $\alpha_{Cl4CH8}=108.17$, $\tau_{Cl4CCCl3}=66.48$	
	Conf = *sc* Sym = C_1	$r_{CC}=1.5748$, $r_{CCl3}=1.7895$, $r_{CCl4}=1.7902$, $r_{CF5}=1.3393$, $r_{CF6}=1.3538$, $r_{CF7}=1.3546$, $r_{CH8}=1.0982$, $\alpha_{CCCl3}=112.38$, $\alpha_{CCCl4}=111.92$, $\alpha_{CCF5}=112.70$, $\alpha_{CCF6}=106.95$, $\alpha_{CCF7}=111.68$, $\alpha_{CCH8}=107.07$, $\alpha_{Cl3CF5}=108.68$, $\alpha_{Cl3CF6}=108.75$, $\alpha_{Cl4CF7}=109.41$, $\alpha_{Cl4CH8}=107.37$, $\tau_{Cl4CCCl3}=-122.47$	
$CClF_2$–$CClF_2$	Conf = *ap* Sym = C_{2h}	$r_{CC}=1.5583$, $r_{CCl}=1.7908$, $r_{CF}=1.3401$, $\alpha_{CCCl}=110.39$, $\alpha_{CCF}=109.44$, $\alpha_{FCF}=108.83$	132.166
	Conf = *sc* Sym = C_2	$r_{CC}=1.5608$, $r_{CCl}=1.7840$, $r_{CF5,7}=1.3445$, $r_{CF6,8}=1.3401$, $\alpha_{CCCl}=112.03$, $\alpha_{CCF5,7}=107.67$, $\alpha_{CCF6,8}=109.41$, $\alpha_{ClCF5,7}=109.32$, $\alpha_{ClCF6,8}=110.02$, $\tau_{ClCCCl}=65.40$	
$CClF_2$–CCl_2F	Conf = *ap* Sym = C_s	$r_{CC}=1.5686$, $r_{CCl3}=1.7828$, $r_{CF4}=1.3508$, $r_{CF5,6}=1.3428$, $r_{CCl7,8}=1.7858$, $\alpha_{CCCl3}=113.27$, $\alpha_{CCF4}=106.25$, $\alpha_{CCF5,6}=108.19$, $\alpha_{CCCl7,8}=110.84$, $\alpha_{F5CF6}=107.96$, $\alpha_{Cl7CCl8}=111.31$	156.163
	Conf = *sc* Sym = C_1	$r_{CC}=1.5662$, $r_{CCl3}=1.7901$, $r_{CF4}=1.3454$, $r_{CF5}=1.3384$, $r_{CF6}=1.3422$, $r_{CCl7}=1.7942$, $r_{CCl8}=1.7858$, $\alpha_{CCCl3}=111.29$, $\alpha_{CCF4}=108.39$, $\alpha_{CCF5}=109.95$,$\alpha_{CCF6}=108.64$, $\alpha_{CCCl7}=108.96$, $\alpha_{CCCl8}=110.82$, $\alpha_{Cl3CF5}=109.70$, $\alpha_{Cl3CF6}=108.63$, $\alpha_{F4CCl7}=108.78$, $\alpha_{F4CCl8}=109.54$, $\alpha_{Cl3CCF4}=57.08$	

possessing at least one threefold symmetrical group. For molecules having two asymmetrical rotational groups, the reduced moment of inertia was approximated by Eq. (4) and calculated individually for each rotational conformation. The value for the molecule was taken as the mean value of the rotational isomers according to the statistical weight of the isomers. The contributions were then calculated numerically [3]. Although this seems to be a rough approximation, good prediction of the heat capacity is achieved, as will be seen later.

In Table II the vibrational frequencies obtained from the B3LYP/cc-pVDZ method are given. No comparison is made to observed fundamentals from the literature, since assignments were proven to be erroneous to some extent in an earlier paper [8]. For the vibrational contribution to the heat capacity of the molecules possessing different rotational isomers, a mean value was taken according to their statistical weight.

To obtain the intramolecular potential energy of hindered internal rotation, we performed single-point B3LYP/cc-pVDZ calculations with the molecular geometry from Table I while varying the torsional angle of the CC axis. In the same way we performed MP2/cc-pVTZ calculations for the energy differences of the rotational isomers. As can be seen from Table III,

Table II. Calculated Vibrational Frequencies (cm^{-1})

C_2H_6		CH_3–CHF_2		CH_3–CF_3		CH_3–CF_2Cl		CH_3–$CFCl_2$		CF_3–CH_2F	
A_{1g}	3028	A′	3141	A_1	3069	A′	3150	A′	3168	A′	3059
	1410		3054		1417		3062		3059		1462
	1011		3050		1284		1450		1448		1435
A_{2u}	3026		1455		827		1400		1393		1300
	1386		1420		593		1240		1129		1185
E_g	3082		1370	E	3161		1120		1118		1111
	1474		1151		1453		896		935		837
	1204		1141		1238		662		577		654
E_u	3107		872		966		538		426		540
	1477		562		532		417		371		404
	821		461		358		300		254		211
		A″	3139			A″	3170	A″	3144	A″	3120
A_{1u}	317^a		1458	A_2	222^a		1449		1448		1304
			1374				1213		1093		1192
			1147				970		716		970
			947				423		389		523
			376				326		293		345
			237^a				242^a		269^a		96^a

Table II. *(Continued)*

CF_3–CH_2Cl		CF_3–CHF_2		CF_3–$CHClF$		CF_3–$CHCl_2$		CF_3–$CClF_2$	
A′	3103	A′	3085	A	3115	A′	3146	A′	1345
	1441		1434		1383		1325		1234
	1338		1310		1299		1281		1126
	1270		1196		1280		1145		957
	1157		1137		1218		866		749
	849		860		1162		755		640
	785		713		1118		663		545
	630		571		871		518		426
	529		514		801		372		357
	350		356		687		257		309
	181		236		564		207		178
A″	3172	A″	1363		521	A″	1220	A″	1251
	1298		1222		442		1196		1199
	1105		1147		369		806		585
	900		574		314		548		443
	526		407		231		348		323
	345		202		182		181		210
	93[a]		60[a]		65[a]		66[a]		55[a]

CF_2Cl-CF_2Cl				CF_2Cl-$CFCl_2$				CF_2Cl-$CHClF$			
									Ap	+sc	−ac
A_g	1280	A	1274	A′	1214	A	1221	A	3123	3122	3100
	1027		1193		1107		1204		1358	1354	1355
	696		1027		1025		1139		1269	1270	1270
	425		668		865		1029		1252	1248	1191
	353		484		624		874		1175	1148	1171
	248		427		496		786		1123	1100	1126
A_u	1215		321		427		649		967	977	1055
	367		304		365		524		790	829	829
	215		165		301		448		764	790	646
B_g	1203	B	1202		247		428		619	591	622
	533		1120		164		385		472	443	490
	315		893	A″	1186		345		420	418	422
B_u	1144		614		868		309		384	399	418
	814		435		446		283		337	321	329
	601		395		374		237		259	305	305
	423		303		304		196		233	224	196
	163		198		176		161		167	163	168
A_u	53[a]	A	63[a]		68[a]		65[a]		63[a]	69[a]	69[a]

[a] Torsional mode.

Table III. Relative Energy Differences and Potential Coefficients (kcal·mol^{-1})

Molecule	Method	$\Delta E_{\text{ap–ac}} = V_3$	$\Delta E_{\text{ap–"30°"}}$	V_6
C_2H_6	MP2/cc-pVTZ	2.91	1.46	0.005
	B3LYP/cc-pVDZ	2.93	—	—
CH_3–CHF_2	MP2/cc-pVTZ	3.35	1.54	−0.135
	B3LYP/cc-pVDZ	3.20	—	—
CH_3–CF_3	MP2/cc-pVTZ	3.27	1.63	−0.005
	B3LYP/cc-pVDZ	2.90	—	—
CH_3–$CClF_2$	MP2/cc-pVTZ	3.89	1.86	−0.085
	B3LYP/cc-pVDZ	3.50	—	—
CH_3–CCl_2F	MP2/cc-pVTZ	4.68	2.11	−0.230
	B3LYP/cc-pVDZ	4.27	—	—
CF_3–CH_2F	MP2/cc-pVTZ	4.00	1.99	−0.010
	B3LYP/cc-pVDZ	3.05	—	—
CF_3–CH_2Cl	MP2/cc-pVTZ	4.55	2.33	0.055
	B3LYP/cc-pVDZ	3.61	—	—
CF_3–CHF_2	MP2/cc-pVTZ	3.85	1.77	−0.155
	B3LYP/cc-pVDZ	2.43	—	—
CF_3–$CHClF$	MP2/cc-pVTZ	4.92	2.48	0.020
	B3LYP/cc-pVDZ	3.42	—	—
CF_3–$CClF_2$	MP2/cc-pVTZ	5.37	2.70	0.019
	B3LYP/cc-pVDZ	3.39	—	—
CF_3–$CHCl_2$	MP2/cc-pVTZ	6.00	2.63	−0.370
	B3LYP/cc-pVDZ	4.46	—	—

the relative energy differences between staggered and eclipsed conformations calculated from the B3LYP/cc-pVDZ method are lower than the corresponding MP2/cc-pVTZ values except for C_2H_6. For the molecules possessing at least three atoms of the same kind attached to one carbon atom, we also calculated the relative energy difference between the eclipsed conformation and a rotation of 30° around the CC axis. This leads to the V_6 coefficient of the series expansion affecting the shape of the potential energy of internal rotation in the intermediate region between staggered and eclipsed conformations.

The relative energy differences of the molecules possessing two asymmetrical rotational groups are presented in Table IV. The coefficients V_n of the series expansion of the potential energy [cf. Eq. (4)], were obtained from a fit to these relative energy differences and are given in Table V. An exact reproduction of the relative energy differences from this representation was achieved for R114. For R113 and R123a, the maximum deviation of 1 kJ·mol^{-1} between the calculated relative energy differences and the series expansion is observed for R113 and is considered negligible relative to the largest value of 38.66 kJ·mol^{-1} and the approximation of

Table IV. Relative Energy Differences of the Molecules Possessing Two Asymmetrical Rotational Groups (kcal·mol^{-1})

Molecule	Method	ΔE_{ap}	$\Delta E_{+\mathrm{ac}}/\Delta E_{-\mathrm{ac}}$	$\Delta E_{+\mathrm{sc}}/\Delta E_{-\mathrm{sc}}$	ΔE_{sp}
$CClF_2$–CHClF	MP2/cc-pVTZ	0.13	5.91/5.90	0.36/0.00	7.06
	B3LYP/cc-pVDZ	0.00	4.37/4.17	0.67/0.20	6.05
$CClF_2$–$CClF_2$	MP2/cc-pVTZ	0.00	6.67	0.37	7.71
	B3LYP/cc-pVDZ	0.00	4.51	0.63	6.50
$CClF_2$–CCl_2F	MP2/cc-pVTZ	0.26	9.24	0.00	7.91
	B3LYP/cc-pVDZ	0.72	7.47	0.00	5.44

the reduced moment of inertia. Moreover, the shape of the potential energy in the intermediate regions between these conformations was also considered to be negligible for the same reasons.

In the following we compare our calculated results to experimental heat capacity data extrapolated to zero pressure (cf. Figs. 1 to 14). In these departure plots the B3LYP/cc-pVDZ calculations with the contribution of hindered internal rotation evaluated from MP2/cc-pVTZ energies are chosen as a reference. As shown in these figures, an uncertainty of ±1.5% or less is achieved for the predictions. If only a threefold V_3 coefficient is taken into account, a heat capacity is obtained which is nearly up to 0.4% higher (cf. the solid lines). For molecules possessing asymmetrical rotating groups, a single V_3^* term was estimated from regression analysis (cf. the last column in Table V). If only such an "effective" potential term is taken into account, the predictions move closer to the experimental data. But due to the underlying assumptions, not too much importance should be attached to this result. It shows, however, that good agreement may also be obtained from one effective threefold term. As mentioned earlier, the

Table V. Potential Coefficients V_n Estimated from Relative Energy Differences in Table IV (kcal·mol^{-1})

Molecule	Method	V_1	V_2	V_3	V_4	V_5	V_3 [a]
$CClF_2$–CHClF	MP2/cc-pVTZ	0.736	−0.431	6.171	−0.216	0.147	6.290
	B3LYP/cc-pVDZ	1.231	−0.598	4.573	−0.299	0.246	—
$CClF_2$–$CClF_2$	MP2/cc-pVTZ	0.783	−0.298	6.770	−0.149	0.157	8.797
	B3LYP/cc-pVDZ	1.456	−0.604	4.753	−0.302	0.291	—
$CClF_2$–CCl_2F	MP2/cc-pVTZ	−0.739	0.591	8.797	0.296	−0.148	7.017
	B3LYP/cc-pVDZ	−1.128	0.902	6.793	0.451	−0.226	—

[a] Only a threefold symmetrical coefficient was considered and estimated from regression of the relative energies.

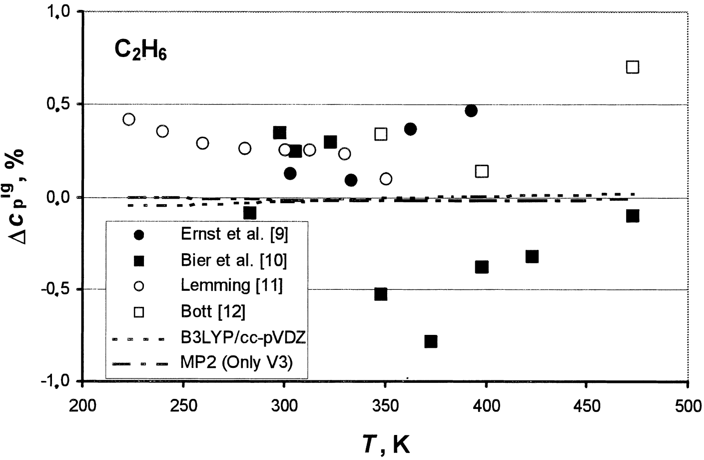

Fig. 1. Experimental and predicted heat capacity of C_2H_6. Reference line: heat capacity calculated from B3LYP/cc-pVDZ//MP2/cc-pVTZ.

B3LYP/cc-pVDZ method leads to relative energy differences of the isomers, which are smaller than those from single-point MP2/cc-pVTZ calculations. If the contribution of hindered internal rotation is evaluated with B3LYP/cc-pVDZ energies, the results shown as dashed lines in the figures are obtained. It is observed that these energies lead to heat capacities which are up to nearly 1% higher than the reference data. Obviously, the B3LYP/cc-pVDZ method is well suited for the prediction of vibrational frequencies, whereas MP2/cc-pVTZ is more adequate for the prediction of energy differences in hindered internal rotation. This empirical result is not inconsistent within the theoretical basis of the calculations, because for the calculation of vibrational frequencies, the second partial derivatives of the potential energy at equilibrium with respect to coordinates of the nuclei are required, i.e., the shape of the potential is the decisive factor, and not the energy value itself as for internal rotation.

4. CONCLUSION

We performed B3LYP/cc-pVDZ calculations for all fluorochloroderivatives of methane and ethane. From the results we obtained, we conclude that the B3LYP/cc-pVDZ method is well suited for the prediction of vibrational frequencies and their contribution to the ideal gas state functions. For satisfactory prediction of the ethane-like molecules, it is evident that additional MP2/cc-pVTZ calculations have to be performed to get accurate coefficients of the potential energy of hindered internal

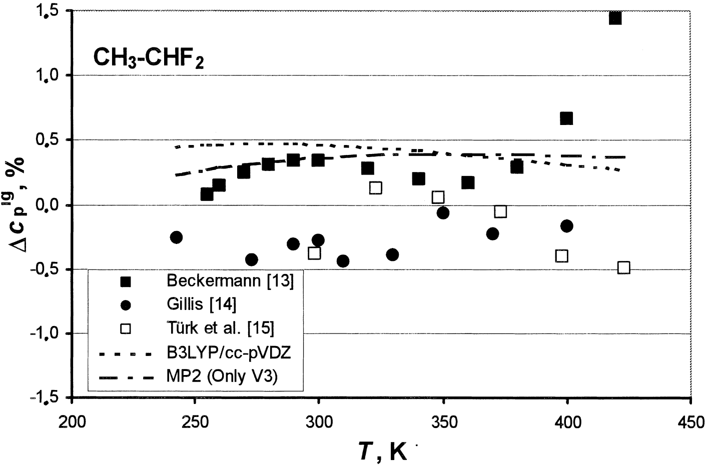

Fig. 2. Experimental and predicted heat capacity of CH_3–CHF_2 (R152a). Reference line: heat capacity calculated from B3LYP/cc-pVDZ//MP2/cc-pVTZ.

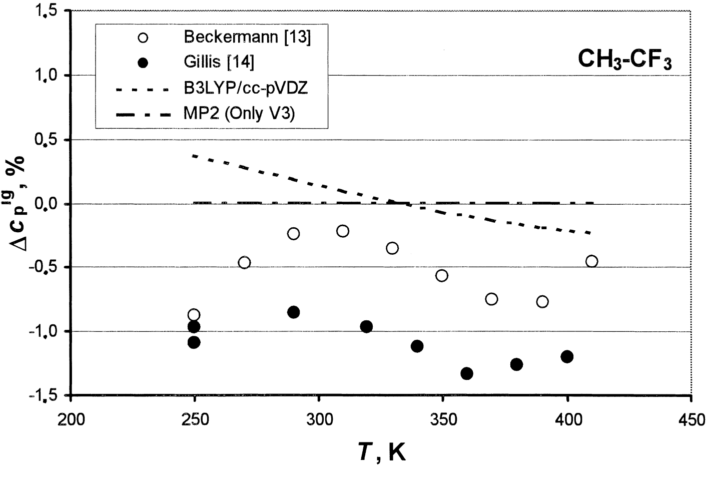

Fig. 3. Experimental and predicted heat capacity of CH_3–CF_3 (R143a). Reference line: heat capacity calculated from B3LYP/cc-pVDZ//MP2/cc-pVTZ.

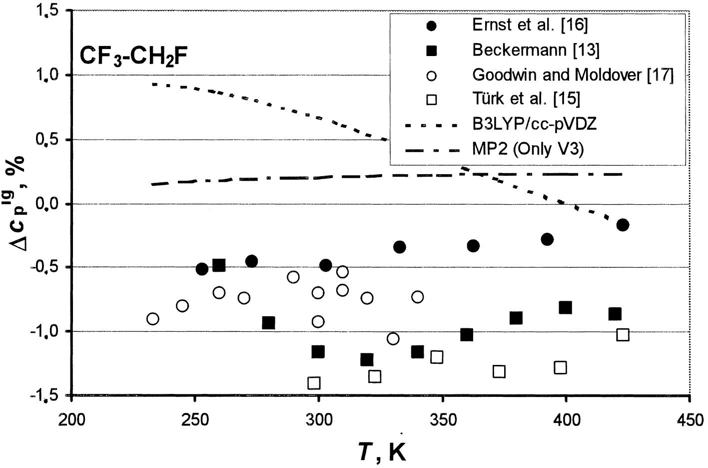

Fig. 4. Experimental and predicted heat capacity of CF_3–CH_2F (R134a). Reference line: heat capacity calculated from B3LYP/cc-pVDZ//MP2/cc-pVTZ.

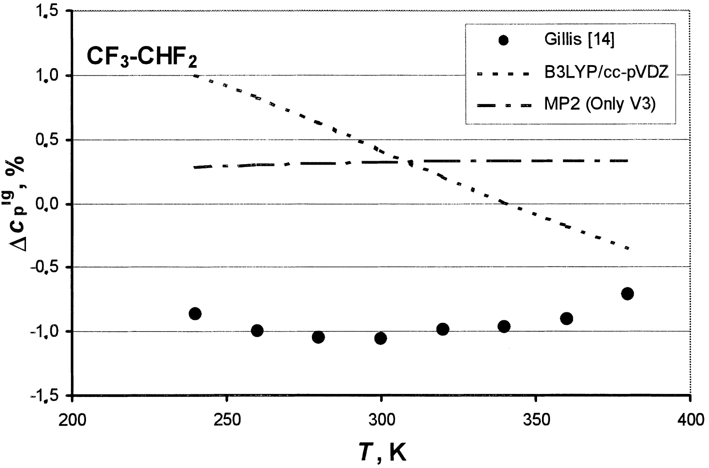

Fig. 5. Experimental and predicted heat capacity of CF_3–CHF_2 (R125). Reference line: heat capacity calculated from B3LYP/cc-pVDZ//MP2/cc-pVTZ.

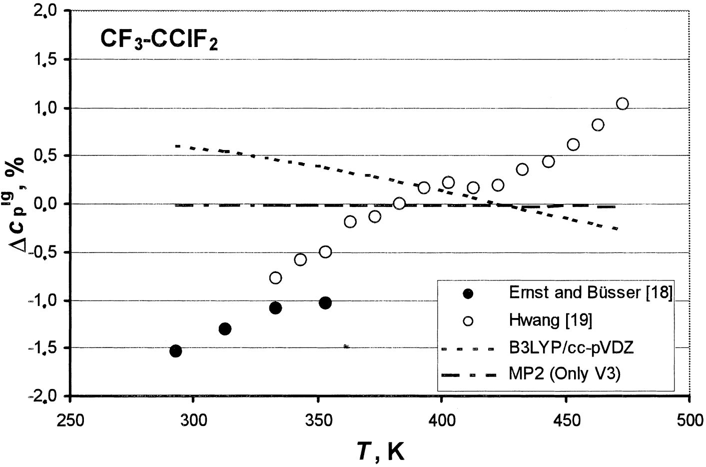

Fig. 6. Experimental and predicted heat capacity of CF_3–$CClF_2$ (R115). Reference line: heat capacity calculated from B3LYP/cc-pVDZ//MP2/cc-pVTZ.

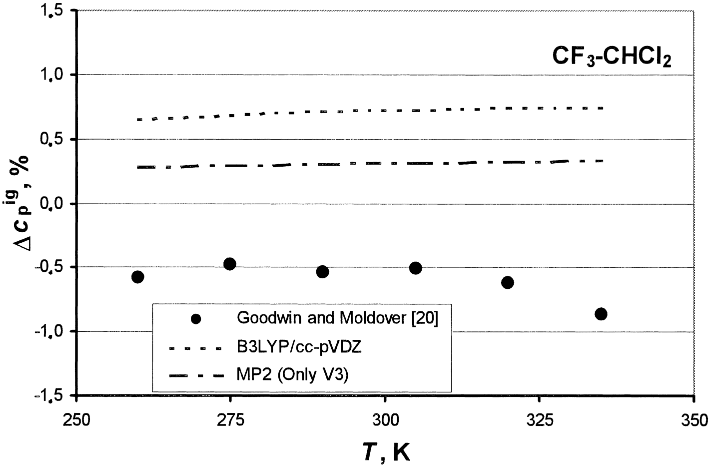

Fig. 7. Experimental and predicted heat capacity of CF_3–$CHCl_2$ (R123). Reference line: heat capacity calculated from B3LYP/cc-pVDZ//MP2/cc-pVTZ.

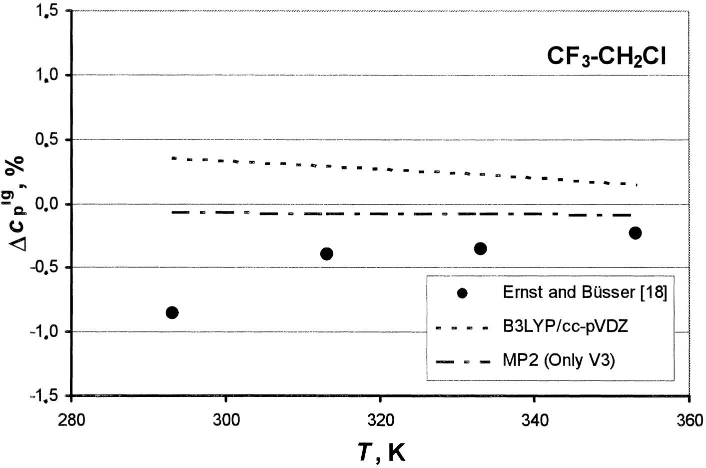

Fig. 8. Experimental and predicted heat capacity of CF_3–CH_2Cl (R133a). Reference line: heat capacity calculated from B3LYP/cc-pVDZ//MP2/cc-pVTZ.

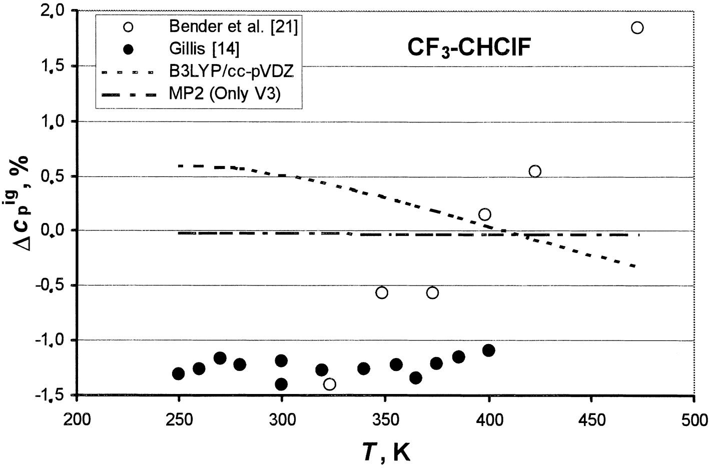

Fig. 9. Experimental and predicted heat capacity of CF_3–CHClF (R124). Reference line: heat capacity calculated from B3LYP/cc-pVDZ//MP2/cc-pVTZ.

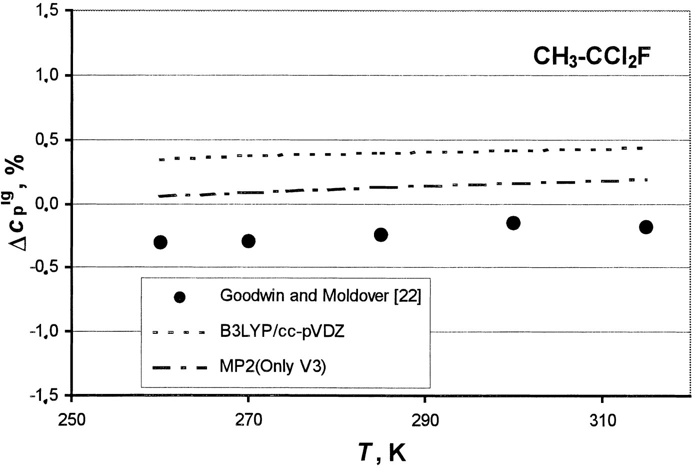

Fig. 10. Experimental and predicted heat capacity of CH_3–CCl_2F (R141b). Reference line: heat capacity calculated from B3LYP/cc-pVDZ//MP2/cc-pVTZ.

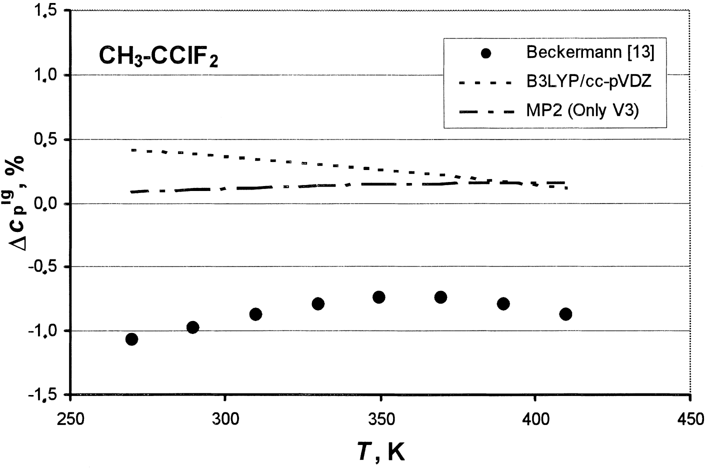

Fig. 11. Experimental and predicted heat capacity of CH_3–$CClF_2$ (R142b). Reference line: heat capacity calculated from B3LYP/cc-pVDZ//MP2/cc-pVTZ).

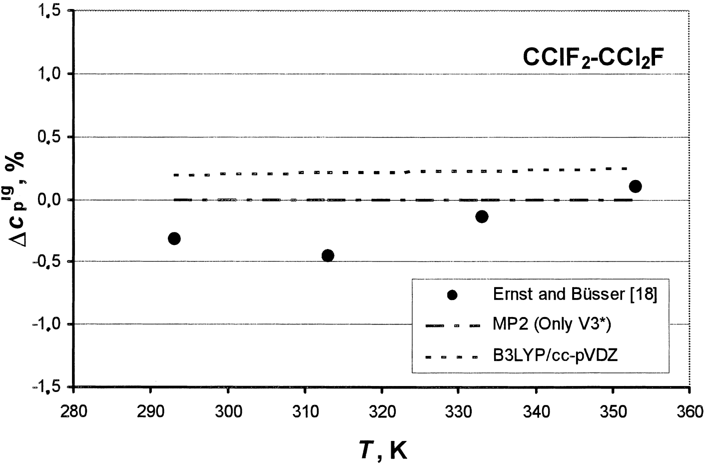

Fig. 12. Experimental and predicted heat capacity of $CClF_2$–CCl_2F (R113). Reference line: heat capacity calculated from B3LYP/cc-pVDZ//MP2/cc-pVTZ.

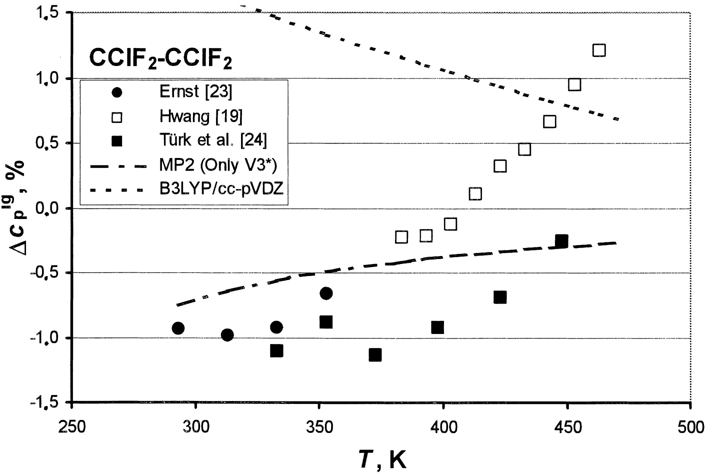

Fig. 13. Experimental and predicted heat capacity of $CClF_2$–$CClF_2$ (R114). Reference line: heat capacity calculated from B3LYP/cc-pVDZ//MP2/cc-pVTZ.

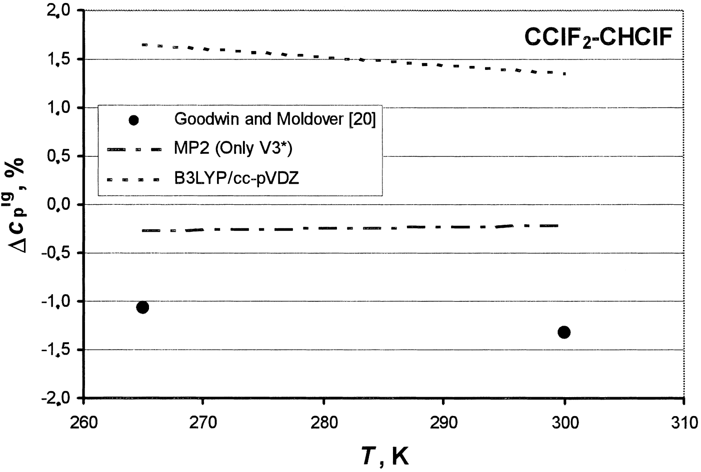

Fig. 14. Experimental and predicted heat capacity of $CClF_2$–CHClF (R123a). Reference line: heat capacity calculated from B3LYP/cc-pVDZ//MP2/cc-pVTZ.

rotation. Finally, reliable experimental heat capacity data reveal that, for the methane-like molecules considered in the previous paper [2] and the derivatives of ethane presented here, an uncertainty of $\pm 1.5\%$ or less is achieved. Therefore, the combination of quantum mechanics and statistical thermodynamics provides a rational and reliable method for prediction of ideal gas heat capacities.

ACKNOWLEDGMENT

M. Speis acknowledges financial support by the Deutsche Forschungsgemeinschaft.

NOMENCLATURE

c_p	Molar heat capacity at constant pressure
c	Contribution to heat capacity
I	Moment of inertia
N	Number of atoms in a molecule
R	Molar gas constant
T	Thermodynamic temperature
V_{ir}	Potential energy of internal rotation
V_n	nth coefficient of the series expansion

Greek Symbols

φ	Torsional angle
ν_i	Normal vibrational frequency (anharmonic)

Subscripts

irot	Internal rotation
red	Reduced
rot	External rotation
tr	Translation
vib	Vibration

Superscripts

o	Experimental at zero pressure
ig	Ideal gas

REFERENCES

1. M. Speis, U. Delfs, and K. Lucas, *Fluid Phase Equil.* **170**:285 (2000).
2. M. Speis, U. Delfs, and K. Lucas, *Int. J. Thermophys.* **21**:1197 (2000).
3. K. Lucas, *Applied Statistical Thermodynamics* (Springer-Verlag, Berlin, 1991).
4. P. J. Stevens, F. J. Devlin, C. F. Chablowski, and M. J. Frisch, *J. Phys. Chem.* **98**:11623 (1994).
5. T. H. Dunning, *J. Chem. Phys.* **90**:1007 (1989).
6. M. J. Frisch, G. W. Trucks, H. B. Schlegel, G. E. Scuseria, M. A. Robb, J. R. Cheeseman, V. G. Zakrzewski, J. A. Montgomery, R. E. Stratmann, J. C. Burant, S. Dapprich, J. M. Millam, A. D. Daniels, K. N. Kudin, M. C. Strain, O. Farkas, J. Tomasi, V. Barone, M. Cossi, R. Cammi, B. Mennucci, C. Pomelli, C. Adamo, S. Clifford, J. Ochterski, G. A. Petersson, P. Y. Ayala, Q. Cui, K. Morokuma, D. K. Malick, A. D. Rabuck, K. Raghavachari, J. B. Foresman, J. Cioslowski, J. V. Ortiz, B. B. Stefanov, G. Liu, A. Liashenko, P. Piskorz, I. Komaromi, R. Gomperts, R. L. Martin, D. J. Fox, T. Keith, M. A. Al-Laham, C. Y. Peng, A. Nanayakkara, C. Gonzalez, M. Challacombe, P. M. W. Gill, B. G. Johnson, W. Chen, M. W. Wong, J. L. Andres, M. Head-Gordon, E. S. Replogle, and J. A. Pople, *Gaussian 98 (Revision A.2)* (Gaussian, Inc., Pittsburgh, PA, 1998).
7. K. Lucas and M. Speis, *DFG Abschlussbericht* (Deutsche Forschungsgemeinschaft, Germany, 1999)
8. U. Delfs, *VDI Fortschritt-Berichte, Reihe 19, Nr. 81* (VDI-Verlag, Düsseldorf, Germany, 1995).
9. G. Ernst and U.E. Hochberg, *J. Chem. Thermodyn.* **21**:407 (1989).
10. K. Bier, J. Kunze, G. Maurer, and H. Sand, *J. Chem. Eng. Data* **21**:5 (1976).
11. W. Lemming, *VDI Fortschritt-Berichte, Reihe 19, Nr. 32* (VDI-Verlag, Düsseldorf, Germany, 1989).
12. T. Bott, Dissertation (Universität Fridericiana, Karlsruhe, Germany, 1986).

13. W. Beckermann, *VDI Fortschritt-Berichte, Reihe 19, Nr. 67* (VDI-Verlag, Düsseldorf, Germany, 1993).
14. K. A. Gillis, *Int. J. Thermophys.* **18**:73 (1997).
15. M. Türk, M. Crone, and K. Bier, *J. Chem. Thermodyn.* **28**:1179 (1996).
16. G. Ernst, J. Gürtner, and H. J. Wirbser, *Chem. Thermodyn.* **29**:1113 (1997).
17. A. R. H. Goodwin and M. R. Moldover, *J. Chem. Phys.* **93**:2741 (1990).
18. G. Ernst and J. Büsser, *J. Chem. Thermodyn.* **2**:787 (1970).
19. Y. T. Hwang, Ph. D. Thesis, University of Michigan, Ann Arbor, Michigan, Microfilm 61-6370.
20. A. R. H. Goodwin and M. R. Moldover, *J. Chem. Phys.* **95**:5236 (1991).
21. K. Bender, K. Bier, and G. Maurer, *J. Chem. Thermodyn.* **12**:335 (1980).
22. A. R. H. Goodwin and M. R. Moldover, *J. Chem. Phys.* **95**:5230 (1991).
23. G. Ernst, *Chemie-Ing.-Techn.* **41**:544 (1969).
24. M. Türk and K. Bier, *VDI Fortschritt-Berichte, Reihe 3, Nr. 331* (VDI Verlag, Düsseldorf, Germany, 1993).